Biological properties of modified bioactive glass on dental pulp cells

Ningxin Zhu[a], Xanthippi Chatzistavrou[b], Lihong Ge[a], Man Qin[a], Petros Papagerakis[c], Yuanyuan Wang[a,*]

[a] Department of Pediatric Dentistry, School and Hospital of Stomatology, Peking University, #22 Zhongguancun Nandajie, Haidian District, Beijing, 100081, China
[b] Michigan State University, Department of Chemical Engineering and Materials Science, East Lansing 48824, MI, USA
[c] College of Dentistry and Biomedical Engineering, Toxicology, Pharmacy/Nutrition, Anatomy and Cell Biology Colleges Graduate Programs, University of Saskatchewan, Canada

ARTICLE INFO

ABSTRACT

Dental caries is a bacteria-caused condition classified among the most common chronic diseases worldwide. Treatment of dental caries implies the use of materials having regenerative and anti-bacterial properties, and controlling inflammation is critical for successful endodontic regeneration.

Objectives: The aim of this study was to fabricate and characterize a novel composite incorporating sol-gel derived silver-doped bioactive glass (BG) in a chitosan (CS) hydrogel at a 1:1 wt ratio(Ag-BG/CS).

Methods: The effect of Ag-BG/CS on dental pulp cells (DPCs) proliferation was analyzed by CCK-8 assay, whereas the adhesion of DPCs was evaluated by confocal microscopy. The physical morphology of Ag-BG/CS was analyzed by scanning electron microscope. The anti-inflammatory effect of Ag-BG/CS was investigated by quantitative polymerase chain reaction (qPCR). Moreover, the effect of Ag-BG/CS on odontogenic differentiation of DPCs was studied by immunochemical staining, tissue-nonspecific alkaline phosphatase staining, qPCR, and western blot analyses. The antibacterial activity against dental caries key pathogenic bacteria was also evaluated.

Results: The results of this study showed that Ag-BG/CS did not affect the proliferation of DPCs, it downregulated the inflammatory-associated markers (IL-1β, IL-6, IL-8, TNF-α) of DPCs treated with *Escherichia coli* lipopolysaccharide (LPS) by inhibiting NF-κB pathway, and enhanced the *in vitro* odontogenic differentiation potential of DPCs. Furthermore, Ag-BG/CS strongly inhibited *Streptococcus mutans* and *Lactobacillus casei* growth.

Conclusions: This novel biomaterial possessed antibacterial and anti-inflammatory activity, also enhanced the odontogenic differentiation potential of LPS-induced inflammatory-reacted dental pulp cells. The material introduced in this study may thus represent a suitable dental pulp-capping material for future clinical applications.

1. Introduction

Dental pulp vitality is essential for root development in immature permanent teeth and reparative dentin formation to respond to external cues. Vital pulp therapy (VPT) is an effective approach to protect the injured pulp, in order to reduce inflammation and promote formation of reparative hard tissue that shields the pulp tissue from injurious agents. An ideal pulp-capping material should stimulate tertiary reparative dentinogenesis and possess biocompatibility, bactericidal, and anti-inflammatory capabilities, among the others [1]. Besides calcium hydroxide and mineral trioxide aggregate (MTA), which are the most common pulp-capping materials, a variety of materials, including bioactive ones, have been investigated in recent studies (Appendix. Table 1). However, no ideal dental pulp capping material for the repair of inflamed pulp has been identified to date.

Following the synthesis of 45S5 Bioglass® [2] by Hench and coworkers, many *in vitro* and *in vivo* studies carried out in the recent decades confirmed bioglass as a bioactive material capable of bonding to mineralized and soft tissue [2–5]. Silver is a common element used in medical materials together with bioglass, due to its established antibacterial activity [6,7]. Ag-doped bioactive glass (Ag-BG) was fabricated and confirmed strong bonding to dentin [8], and demonstrated the odontogenic properties *in vivo* [9]. Chitosan (CS)-based thermogelling solution, which undergoes sol-gel transition upon temperature increase, possesses multiple intrinsic properties such as biocompatibility and bacteriostatic effects [10]. It has been extensively

investigated in the past decade [11] and offered more predictable hydrogel properties. Here, CS was added to Ag-BG materials to enhance their operability as dental pulp capping agents. The hypothesis of the study was that this novel biomaterial possessed antibacterial and anti-inflammatory activity, also enhanced the odontogenic differentiation potential of inflamed dental pulp cells. The purpose of this study is to evaluate the biological properties of a hybrid system produced by incorporating Ag-BG into injectable chitosan hydrogel(Ag-BG/CS).

2. Materials and methods

2.1. Synthesis of Ag-BG/CS gel

Ag-doped bioactive glass micro-size particles were provided by Professor Papagerakis from University of Saskatchewan, they were fabricated according to a previously reported procedure [12]. Briefly, the fabrication protocol was on the basis of the sol-gel process by mixing the solution stage of the 58S sol-gel bioactive glass (in the system SiO_2 58-CaO 33-P_2O_5 9 wt.%), with the respective solution stage of the sol-gel glass in the system SiO_2 60-CaO 6-P_2O_5 3-Al_2O_3 14-Na_2O 5-K_2O 5- Ag_2O 7 wt.%. The mix was stirred and heated as below: aging at 60 °C, drying at 180 °C and stabilization up to 700 °C. The fabricated material was in powder form with particle size < 35 μm. Chitosan hydrogel was provided by department of dental materials in Peking University School and Hospital of Stomatology. The micro-size particles were added into liquid chitosan gel (CS-gel) at a 1:1 wt ratio, mixed adequately at room temperature, forming Ag-BG/CS. The liquid gel was also cast into 0.32 cm^2 × 1 mm cylindrical molds and freeze-dried. The morphology of freeze-dried hydrogel was analyzed by scanning electron microscope (EVO18, Carl Zeiss, Germany). Ag-BG/CS extract liquid was fabricated by soaking freeze-dried Ag-BG/CS in isovolumetric sterile α-modified minimum essential medium (α-MEM, GIBCO/BRL) for 24 h.

2.2. Cell culture

Ethics Committee of the Peking University Health Science Center had reviewed and approved collection of human dental pulp cells (DPCs) from 14 to 18 years old patients that underwent teeth extraction as part of orthodontic treatment. Normal human premolars (n = 3) were collected and all extracted teeth were used for isolating human DPCs. Totally three different teeth were collected and three different DPC primary cell lines were generated and examined following the exact same procedures and methods. Results obtained from the three different DPCs cultures were similar. DPCs were isolated from the dental pulp space and then digested in 3 mg/mL type I collagenase (Sigma-Aldrich, St. Louis, MO, USA) and 4 mg/mL dispase (Sigma-Aldrich, St. Louis, MO, USA) for 1 h at 37 °C. Next, the DPC suspensions were separated using a 70 μm strainer (Falcon, BD Biosciences, San Jose, CA, USA). The single-cell suspensions were cultured in α-modified minimum essential medium (α-MEM, GIBCO/BRL) with 10% fetal bovine serum (FBS, GIBCO), 100 U/mL penicillin, and 100 μg/mL streptomycin at a 37 °C with 5% CO_2 incubator. DPCs between the fourth and sixth passage were used for this study.

2.3. Cell proliferation assay

The influence of Ag-BG/CS on DPCs proliferation was evaluated. DPCs were seeded in 96-well plates (5 × 10^3 cells/well; expanded *ex vivo*), treated with Ag-BG/CS extract liquid, and untreated DPCs as the control group. At 1, 3, 5, 7 days after cell seeding, a CCK-8 (Dojindo, Beijing) assay was carried out with three replications to evaluate the number of viable cells.

2.4. Cell adhesion analysis

The adhesion of the DPCs was assessed by fluorescence staining.

Twelve freeze-dried Ag-BG/CS gels were placed in 24-well plates and DPCs were seeded on Ag-BG/CS (1 × 10^4 cells/well; expanded *ex vivo*), followed by incubation at 37 °C with 5% CO_2. Ag-BG/CS was collected at 6 h, 24 h, and 72 h (Three samples for each point-in-time). Stained viable cell nuclei with 4,6-diamidino-2-phenylindole (DAPI, Invitrogen) staining was then performed in the dark for 5 min. After washed with PBS, the slides were analyzed using a confocal microscope (Zeiss LSM 7 Duo, Germany).

2.5. Quantitative polymerase chain reaction (qPCR)

To induce inflammatory reaction, DPCs were treated with 1 μg/mL *Escherichia coli* lipopolysaccharide (LPS) (Sigma Aldrich, St Louis, MO, USA), produced inflamed dental pulp cells (iDPCs). iDPCs were then treated with Ag-BG/CS extract liquid for 1 h, 3 h, and 6 h. To evaluate odontogenic differentiation potential of the cells, DPCs and iDPCs were cultured in osteogenic media [100 nM dexamethasone, 10 mM sodium β-glycerophosphate, and 50 μg/mL L-ascorbic acid 2-phosphate sesquimagnesium salt hydrate (Sigma-Aldrich, St Louis, MO, USA)] for 7 days.

The relative expression level of inflammatory cytokines and of osteogenic/odontogenic markers was evaluated by quantitative PCR. At the end points, cells were collected and RNA was extracted using TRIzol (Introgen, Carlsbad, CA, USA), 2 μg total RNA was converted to cDNA with Moloney murine leukaemia virus reverse transcriptase (M-MLV RTase, Promega, Madison, WI, USA). Quantitative PCR was carried out in SYBR green master mix (Roche, Indianapolis, IN, USA), with 0.5 μL cDNA and 200 nM of specific primers. Conditions were applied as following: 50 °C for 2 min, then 95 °C for 10 min, followed by 40 cycles of 94 °C for 15 s and 60 °C for 1 min using an ABI PRISM 7500 Sequence Detection System (Applied Biosystems, Foster City, CA, USA). The set of primers used are listed in Table 1. The results were analyzed using the PRISM 6 software (using one-way ANOVA).

2.6. TNAP staining and immunochemical staining

DPCs and iDPCs were seeded in 6-well plates (2 × 10^4 cells/well; expanded *ex vivo*) for alkaline phosphatase (ALP) staining and then treated with Ag-BG/CS extract liquid in osteogenic media for 7 days. ALP levels were determined using the tissue-nonspecific ALP (TNAP) histochemical staining kit (Cwbiotech, Beijing, China). The TNAP staining process was carried out according to the manufacturer's protocol. Briefly, the cells were then fixed in 4% paraformaldehyde for 10 min at room temperature, air-dried, and incubated with substrate for 1 h at 37 °C. Cells were then rinsed with distilled H_2O, air-dried, and visualized macroscopically for evidence of staining. For quantification, 12 wells (three replicates in each group) were scanned, and densitometry was measured using NIH Image J software.

iDPCs, treated with Ag-BG/CS, were subcultured onto 12-chamber slides (2 × 10^4 /well, expanded *ex vivo*) and grown in osteogenic media for 7 days, then the cells were fixed with 4% paraformaldehyde and blocked with phosphate buffered saline (PBS) containing 10% normal bovine serum at room temperature for 45 min. The cells were then incubated with diluted primary antibody osteocalcin (OCN, 1:1000, sc-30044, Santa Cruz, CA, USA) overnight at 4 °C, the immunochemical staining was carried out according to the manufacturer's instructions, 3,3-Diaminobenzidine (DAB) was applied as the chromogen.

2.7. Immunofluorescence

DPCs were plated onto sterile coverslips in 12-well plates and incubated to 40–50% confluence, treated the same as above. Cells were fixed in paraformaldehyde for 10 min, blocked with PBS containing 10% normal bovine serum at room temperature for 2 h. The cells were then incubated with diluted primary antibody p65 (C22B4, 4764 T, Cell Signaling Technology, Danvers, MA, USA) overnight at 4 °C. The coverslips were rinsed with PBS, and then incubated with Rhodamine

Table 1
Primers used for quantitative PCR.

Target gene	Sequence	Product size (bp)	GenBank number
GAPDH	Forward: GCAAATTCCATGGCACCGTC	465	NM_002046.6
	Reverse: GGGGTCATTGATGGCAACAATA		
ALP	Forward: ATGGGATGGGTGTCTCCACA	246	NM_014476.5
	Reverse: CCACGAAGGGGAACTTGTC		
DSPP	Forward: TCCTAGCAAGATCAAATGTGTCAGT	152	NM_014208.3
	Reverse: CATGCACCAGGACACCACTT		
OCN	Forward: AGCAAAGGTGCAGCCTTTGT	261	NM_199173.5
	Reverse: GCGCCTGGGTCTCTTCACT		
RUNX2	Forward: CACTGGCGCTGCAACAAGA	157	NM_001024630.3
	Reverse: CATTCCGGAGCTCAGCAGAATAA		
IL-1β	Forward: TGCACGATGCACCTGTACGA	298	NM_000576.2
	Reverse: AGGCCCAAGGCCACAGGTAT		
IL-6	Forward: ACGAACTCCTTCTCCACAAGC	397	NM_000600.4
	Reverse: CTACATTTGCCGAAGAGCCC		
IL-8	Forward: TTTTGCCAAGGAGTGCTAAAGA	300	BT007067.1
	Reverse: AACCCTCTGCACCCAGTTTTC		
TNF-α	Forward: CAGAGGGAAGAGTTCCCCAG	285	NM_000594.3
	Reverse: CCTCAGCTTGAGGGTTTGCTAC		

(TRITC) Conjugated Goat anti-Rabbit IgG (H + L) (ZF-0316, ZSJQ, China). Nuclei were dyed with DAPI (Solarbio, Beijing, China). Images were captured by a fluorescence microscope (BX51, Olympus, Tokyo, Japan).

2.8. Western blot

DPCs were seeded in 6-well plates (2×10^4 /well) and at 80% confluent were treated with LPS with or without Ag-BG/CS extract liquid for 3 h. At the end points, DPCs were lysed in RIPA buffer with protease inhibitors. Proteins were quantified by BCA Protein Assay (Pierce). Forty micrograms of protein from each sample was separated on 10% SDS-PAGE gels and transferred to PVDF membranes (Millipore, Bedford, MA, USA) at 100 V for 60 min. Then the membranes were bathed in blocking buffer (5% non-fat dry milk in Tris-buffered saline with 0.05% Tween-20, pH 7.4) for 1 h and incubated with the following antibodies at 4 °C overnight: OCN (1:1000, sc-30044, Santa Cruz, CA, USA), runt-related transcription factor 2 (RUNX2, 1:1000, sc-390715, Santa Cruz, CA, USA), p65 (C22B4, 4764 T, Cell Signaling Technology, Danvers, MA, USA), phosphorylated p65 (93H1, 3033 T, Cell Signaling Technology, Danvers, MA, USA) and β-actin (D6A8, 8457 T, Cell Signaling Technology, Danvers, MA, USA). The membranes were incubated in horseradish peroxidase-conjugated secondary antibody (ZSJQ, China) for 1 h at room temperature, and bands were visualized using Fusin Fx (Vilber Lourmat, France).

2.9. Antibacterial assay

Equal volumes of Ag-BG/CS extract liquid or PBS, which was used as the control, were separately mixed with *S. mutans* (ATCC 33342) and *L. casei* (ATCC 53103), and then incubated anaerobically for 24 h at 37 °C; each mixture was subsequently diluted serially (10^{-1}, 10^{-2}, 10^{-3}, 10^{-4} and 10^{-5}) and subsequently was plated on agar plate. The plates were then incubated for 24 h at 37 °C, and the developed colonies were counted.

3. Statistical analysis

The statistical significance of differences within the CCK-8 assay and quantitative PCR results were analyzed by one-way ANOVA (*Dunnett test*) and Student *t*-test using the PRISM 6 software, at significance levels of $p < 0.05^*$, $p < 0.01^{**}$, and $p < 0.001^{***}$.

4. Results

4.1. Effects of Ag-BG/CS on the proliferation of DPCs

The CCK-8 assay was used to investigate the influence of Ag-BG/CS on DPCs proliferation. After treatment with Ag-BG/CS extract liquid, DPCs showed stable growth (Fig. 1B), the proliferation rate was slightly lower compared to control group (Fig. 1B). At day3, 5, 7, there was significantly difference in the numbers of viable cells between two groups ($p < 0.01$) (Fig. 1A).

4.2. Effects of Ag-BG/CS on the adhesion of DPCs

The result of scanning electron microscope(SEM) analysis showed that Ag-BG/CS possessed porous characteristics, with pore diameter reaching around 60–120 μm(Fig. 1C–D). Confocal microscopy measurements revealed that DPCs adhered to Ag-BG/CS within 72 h (Fig. 1E–G), and the cell counting results showed significant differences between amounts of adhesive cells at 6, 24, 72 h (Fig. 1I). The longitudinal view showed that cells could migrate inside the composite and exhibited growth (Fig. 1H).

4.3. Effects of Ag-BG/CS on regulating the inflammatory cytokines expression of iDPCs

According to the quantitative PCR results, the mRNA expression levels of inflammatory cytokines *IL-1β, IL-6, TNF-α, IL-8* in iDPCs showed a marked decrease after treated by Ag-BG/CS ($p < 0.05$) (Fig. 2A–D), all tested cytokine levels showed the significant decrease within 1 h, and rose up at 3 h. The mRNA expression level of *IL-1β* and *IL-6* kept going up under Ag-BG/CS treatment at 6 h (Fig. 2A and B), while the expression of *TNF-α* and *IL-8* were inhibited by Ag-BG/CS 6 h later (Fig. 2C and D).

4.4. Inactivation of NF-κB pathway by Ag-BG/CS treatment

In contrast with control group, after stimulated with LPS for 3 h, p65 translocated into the nucleus, and Bay11-7082 inhibited this procedure. In cells incubated with Ag-BG/CS dilution, nuclear translocation of p65 significantly decreased compared to LPS group (Fig. 2E). Results of western blot showed that phosphated p65 increased under LPS treatment, Bay11-7082 and Ag-BG/CS suppressed the phosphorylation (Fig. 2F). The density of bands was analyzed by ImageJ (Fig. 2G), and differences were significant ($p < 0.05$, one-way ANOVA).
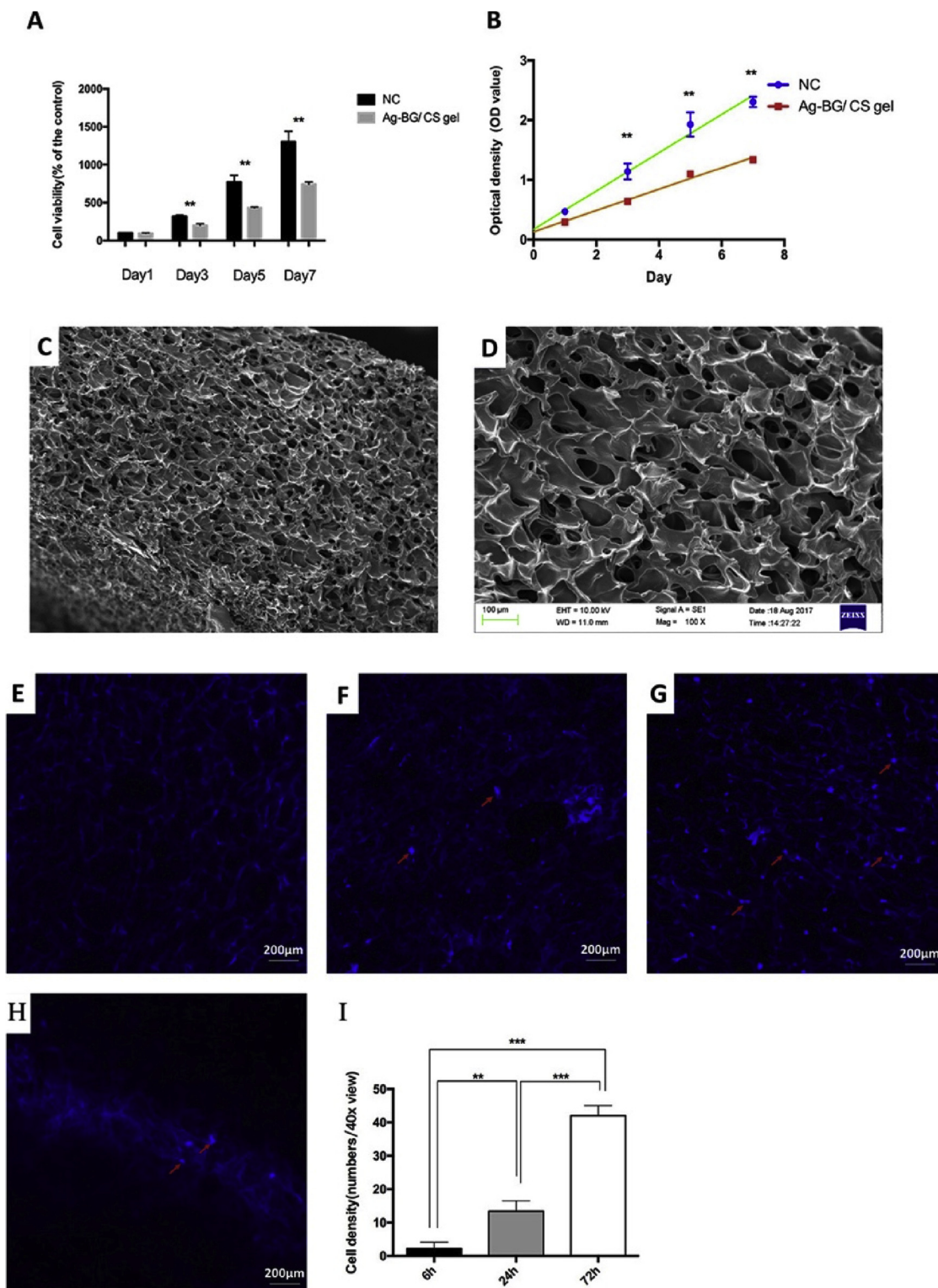
Fig. 1. Cell proliferation rate within 7 days(A) and CCK-8 assay(B) results at 1, 3, 5, 7 days, showed that DPCs grew stably in the Ag-BG/CS group, the 95% confidence interval of the fitted curve slope is 0.1660 to 0.1901, while the slope 95% confidence interval of control group falls in 0.2905 to 0.3498. and at day3, 5, 7, there was significantly differences in amount of viable cells between two groups (p < 0.01) (B). The physical morphology of Ag-BG/CS was observed in Fig. 1C and D. The results of confocal microscope analysis using DAPI-labeled showed DPCs as blue spots (Arrows). Few DPCs can be seen at 6 h(E), whereas a significant amount of DPCs adhered to the Ag-BG/CS gel are visible at 24 h(F) and 72 h(G). The longitudinal view showed that cells could migrate inside the composite and exhibited growth(H). Cell counting results, showing significant differences(I). The asterisks indicated the significance of differences between groups (* p ≤ 0.05, ** p ≤ 0.01, *** p ≤ 0.001, one-way AVONA, *Dunnett* test), and the bars represented the standard deviation of three replicates. The experiment was repeated four times.
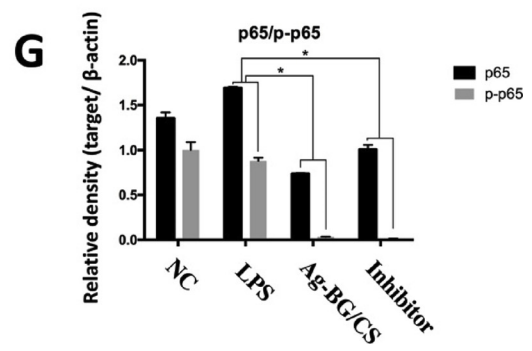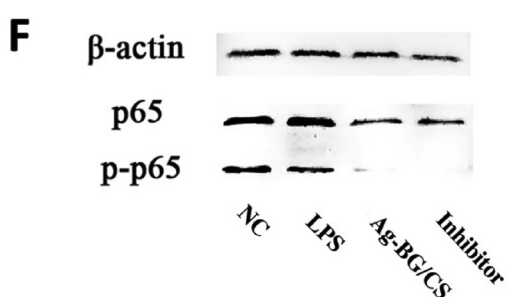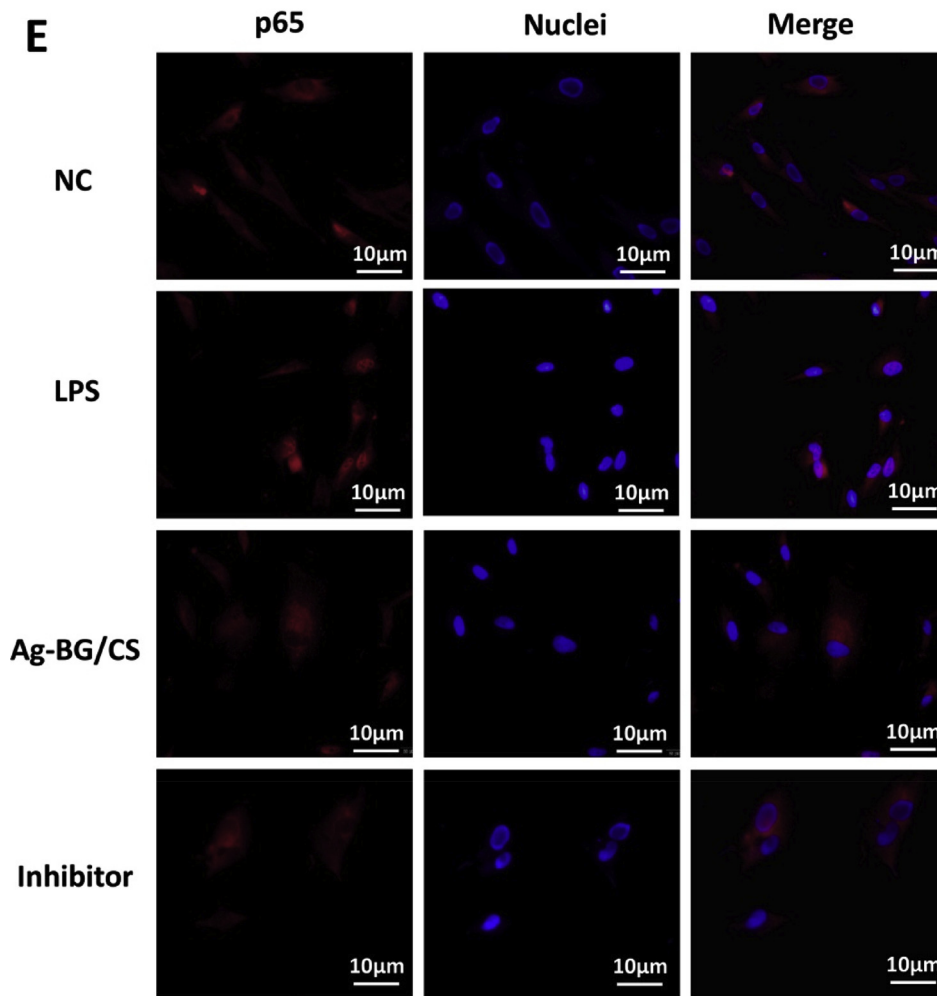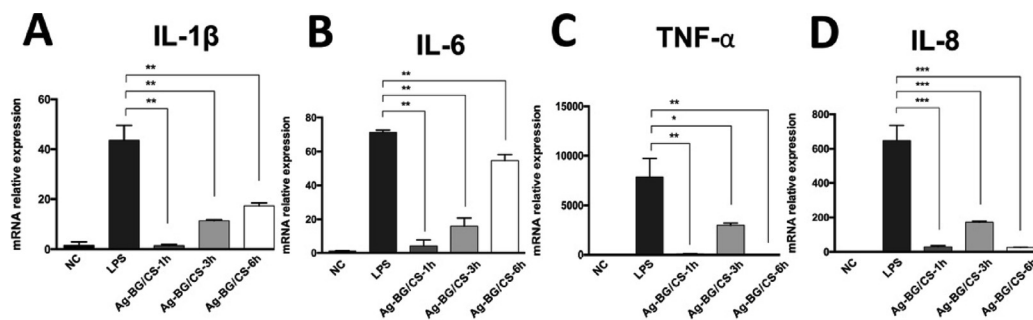
(caption on next page)

Fig. 2. Quantitative PCR analysis, showing significant suppression on the mRNA expression level of *IL-1β, IL-6, IL-8,* and *TNF-α* compared to the iDPCs group(A–D); all tested cytokine levels showed the significant decrease within 1 h, and rebounded at 3 h. The mRNA expression level of *IL-1β*(A) and *IL-6*(B) kept increasing under Ag-BG/CS treatment at 6 h, while the expression of *TNF-α*(C), *IL-8*(D) were inhibited by Ag-BG/CS 6 h later. The asterisks indicated the significance of differences between groups (* $p \leq 0.05$, ** $p \leq 0.01$, *** $p \leq 0.001$, one-way AVONA, *Dunnett* test), and the bars represented the standard deviation of three replicates. After stimulated with LPS for 3 h, p65 translocated into the nucleus, and Bay11-7082 inhibited this procedure. In cells incubated with Ag-BG/CS dilution, nuclear translocation of p65 significantly decreased compared to LPS group(E). Results of Western blot showed that phosphated p65 increased under LPS treatment, Bay11-7082 and Ag-BG/CS suppressed the phosphorylation(F). The density of bands was analysed by ImageJ(G), and differences were significant($p < 0.05$, one-way ANOVA).

4.5. Effects of Ag-BG/CS on the osteo/odontogenic differentiation of iDPCs

The TNAP staining assay was used to evaluate the influence of Ag-BG/CS on mineralization. The ALP activity decreased when DPCs became inflamed, but significantly recovered after treated with Ag-BG/CS, to even higher values compared with non-inflammatory DPCs maintained in the osteogenic medium (Fig. 3B). The osteo/odontogenic differentiation ability was further investigated by examining related biomarkers and their downstream proteins. The immunostaining tests revealed that Ag-BG/CS significantly enhanced the expression of OCN protein (Fig. 3A) in iDPCs. The qPCR analysis showed that Ag-BG/CS significantly increased the expression of *ALP, OCN,* and *RUNX2* at mRNA level ($p < 0.01$) (Fig. 3D), and similar results were obtained with the western blot assay (Fig. 3E).

4.6. Antibacterial properties of Ag-BG/CS against S. mutans and L. casei

The antibacterial properties of the Ag-BG/CS against *S. mutans* and *L. casei* were illustrated. No bacterial growth was observed after 24 h of co-culture with Ag-BG/CS. This difference was statistically significant compared to the PBS co-cultured control group (Fig. 4).

5. Discussion

Dental pulp capping is a common clinical approach aiming to preserve dental pulp tissue and to prevent invasive endodontic procedures [13] that may result in tooth necrosis and tooth loss. Innovative bioactive/biomimetic ion-releasing materials are required for preserving the vitality of dental pulp tissue in immature permanent teeth and primary teeth, by blocking the progress of inflammation and inducing the formation of reparative tissue. DPCs is a mixed population of mesenchymal cells including dental pulp stem cells (DPSCs) and necessary to initiate tertiary dentin formation in response to external stimuli such as caries [14]. The novel material was confirmed combining the different characteristics of its components into a substrate with improved biological properties and it could enhance DPCs properties in defending tissue integrity and regeneration.

The present study highlighted the anti-inflammatory properties of Ag-BG/CS, which reduced the expression of interleukin-1β, -6, and -8 and of tumor necrosis factor-α; these inflammatory cytokines were also suppressed after treatment with chitosan gel alone (Appendix. Fig. 1), suggesting that the anti-inflammatory effect of the material originates from both Ag-BG and chitosan. Chitosan (CS) is an injectable hydrogel; previously used as a drug delivery agent [11], now as an appealing material for dental applications. Moreover, CS possesses strong antibacterial and anti-inflammatory properties [15,16] which may provide additional advantages for dental pulp healing and regeneration under inflammatory conditions. It has been demonstrated that CS was capable of reducing prostaglandin E2 production [17] and suppressing the transcript levels of *IL-6* and *COX-2* genes [18] in human gingival fibroblasts. Interleukins are secreted in dental pulp as a response to bacterial attack [19], whereas TNF-α, as a ligand cytokine, is involved in systemic inflammation [20]. The expression of these cytokines was reduced by Ag-BG/CS, confirming and expanding the findings of previous studies. In our study, Ag-BG/CS inhibited p65 phosphating and translocating into the nucleus, probably inhibited the NF-κB pathway.

Therefore, further investigations are needed to elucidate the cellular and molecular mechanism of the anti-inflammatory activity of Ag-BG/CS.

In this study, Ag-BG/CS was also found to upregulate the expression of multiple osteo/odontogenic markers *in vitro*. BG is a silicate-based bio-glass, capable of inducing mineralized tissue formation when immersed in simulated body fluid (SBF) through induction of nucleation and crystallization of apatite [21]. Ag-BG microsize particles were first fabricated by Chatzistavrou et al., who measured the amount of ions released into suspension, and concluded that the Ag-BG particles could be considered as efficient calcium and silicon sources for re-mineralization [22]. Previous study proposed that calcium ions released from silicate-based materials in addition to be parts of the dentin and bone mineralized matrix were also reported to regulate cell adhesion, enhance odontoblast and osteoblast proliferation and induce cell differentiation [23]. Additionally, previous reports claimed that, in the presence of critical concentrations of silium and calcium ions, osteoblasts were able to differentiate into a mature osteocyte phenotype [24] based on the expression of phenotypic markers such as ALP, RUNX2 and OCN. Soluble $Si(OH)_4$ species had been demonstrated contributing to bone formation *in vitro*, inducing *RUNX2* expression through the NF-κB pathway, and upregulating *OCN* expression [25]. Compared to their inhibited expression in the case of iDPCs, all tested markers, mentioned briefly above, recovered upon treatment with diluted Ag-BG/CS (Fig. 3). Thus, the results indicated that the odontoblastic differentiation potential of the iDPCs was recovered after Ag-BG/CS treatment. In our study, Ag-BG/CS suppressed the phosphorylation and translocation of p65, indicating that Ag-BG/CS probably could inactivate NF-κB pathway. The present results are consistent with previous conclusions. Except for the NF-κB pathway, it had been reported that the odontoblastic potential of DPCs could be enhanced through the activation of the AMPK signaling pathway [14]. Further research is needed to evaluate the exact mechanism controlling the activity of the novel material investigated in this work.

Previous studies showed that Ag-BG had also strong antibacterial properties [6,9,26,27], which had been confirmed in this work. The antibacterial properties of silver ions had been extensively studied and reported in the past 20 years. A previous study showed that silver ions demonstrate a broad-spectrum of antibacterial activity at Ag^+ concentration of 0.4 μg/mL after co-culturing for 24 h [28]. In the case of the material investigated in this work, the released amount of silver ions reached 1.4 μg/mL rapidly within 24 h (data not published), and the present results showed no colonies of *S. mutans* and *L. Casei* observed in the presence of Ag-BG/CS, confirming the bactericidal properties of this material.

6. Conclusion

In the present work, an anti-inflammatory, bactericidal, and re-mineralizing material, consisted of Ag-doped bioactive glass particles incorporated in a chitosan gel, has been proven to be able to suppress the expression of inflammatory cytokines, promote the proliferation and differentiation of iDPCs, and inhibit *S. mutans* and *L. Casei* bacteria growth. The injectable Ag-BG/CS exhibits various bioactive properties and thus represents a promising vital pulp conservation material to improve endogenous DPCs response to dental caries. Detailed
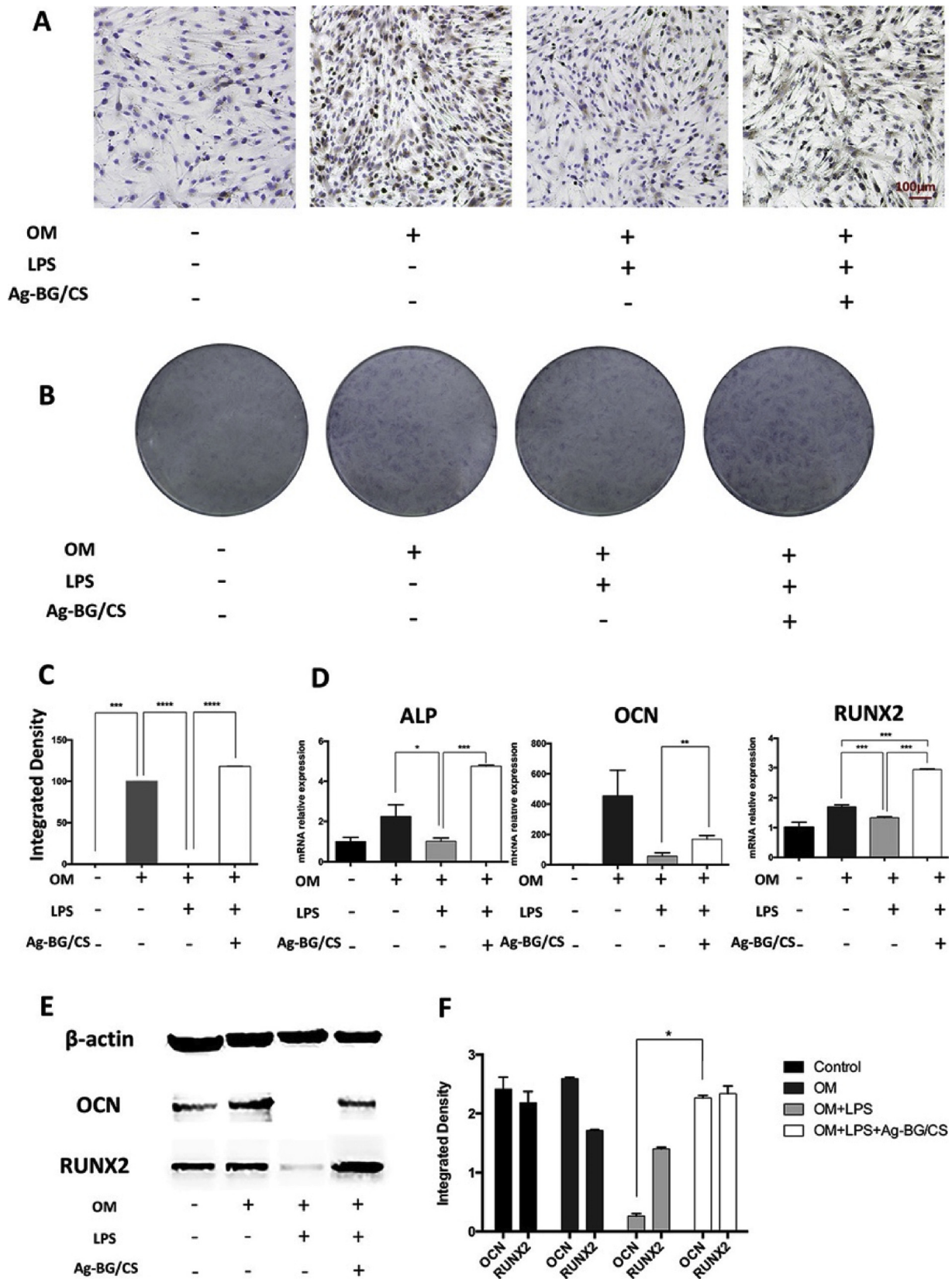
(caption on next page)

Fig. 3. Immunocytochemistry staining analysis and TNAP staining results. Representative images showing OCN (brown) expression of DPCs in extracellular matrix and cell nuclei (blue). Scale bar = 100 μm. Normal DPCs exhibited reduced expression, and osteogenic medium treatment resulted in enhanced OCN expression, iDPCs showed little expression of OCN when grown in osteogenic medium, whereas Ag-BG/CS significantly upregulated the OCN level(A). TNAP staining results(B) showed that the ALP activity was suppressed in the iDPCs (treated with LPS) grown in osteogenic medium (OM) compared to the DPCs grown into OM alone. TNAP expression was recovered in iDPCs treated Ag-BG/CS extract liquid grown in OM. The integrated density of images was analysed using ImageJ (three replicates in each group), and there were significant differences between each two groups(C).

Quantitative PCR analysis, showing significant suppression on the mRNA expression level of *ALP*, *OCN,* and *RUNX2* in the iDPC group compared to osteogenic medium, along with significant recovery in the Ag-BG/CS group (D). Western blot analysis, showing similar results to qPCR, with the expression level of *OCN* and *RUNX2* markedly decreasing in iDPCs group and significantly recovering in the Ag-BG/CS group (E). The density of bands was analysed by ImageJ(F), and differences were significant. The asterisks indicate the significance of differences between groups (* $p \leq 0.05$, ** $p \leq 0.01$, *** $p \leq 0.001$, one-way ANOVA, *Dunnett* test), and the bars represented standard deviations of three replicates.
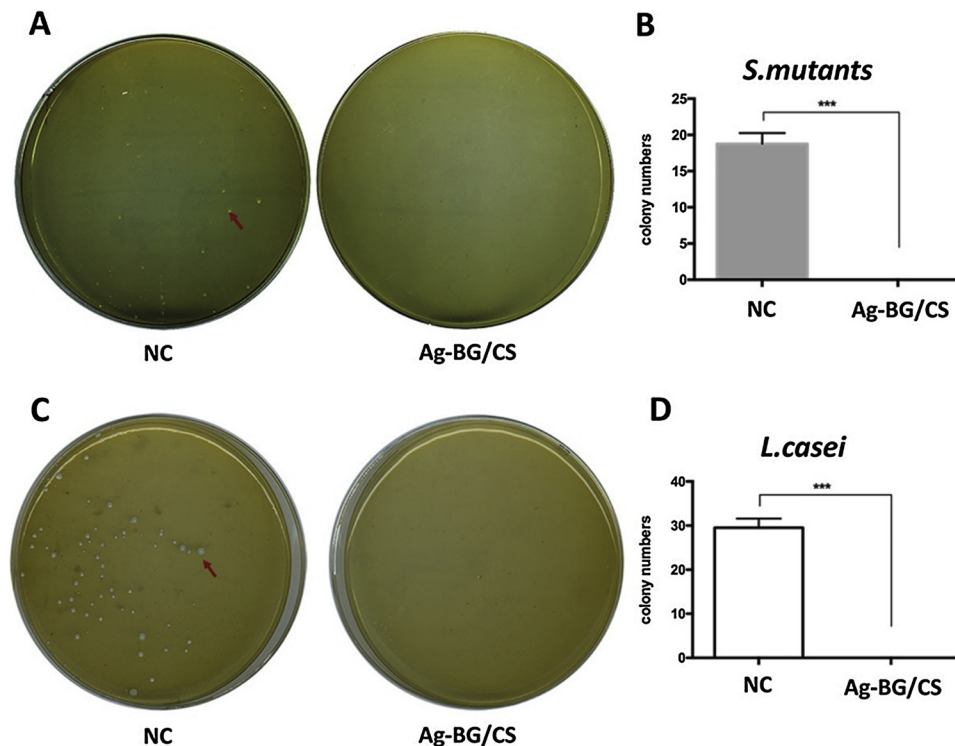

Fig. 4. Antibacterial properties. No colony growth was observed in the presence of the Ag-BG/CS gel, compared to control group (A,C, red arrows showing bacteria colonies); Colony numbers analysis (C) showed that the difference was significant ($p < 0.01$).

investigations of the *in vivo* biological properties of this material are needed to guide its future clinical applications.

Appendix A. Supplementary data

Supplementary material related to this article can be found, in the online version, at doi:https://doi.org/10.1016/j.jdent.2019.01.017.

References

[1] A. Qureshi, S.E. Nandakumar, Pratapkumar Sambashivarao, Recent advances in pulp capping materials: an overview, J. Clin. Diagn. Res. 8 (1) (2014) 316–321.
[2] L. Hench, J. Hench, D. Greenspan, Bioglass: a short history and bibliography, J. Aust. Ceram. Soc. 40 (1) (2004) 1.
[3] A.P. Forsback, S. Areva, J. Salonen, Mineralization of dentin induced by treatment with bioactive glass S53P4 in vitro, Acta Odontol. Scand. 62 (1) (2009) 14–20.
[4] M. Mneimne, R.G. Hill, A.J. Bushby, D.S. Brauer, High phosphate content significantly increases apatite formation of fluoride-containing bioactive glasses, Acta Biomater. 7 (4) (2011) 1827–1834.
[5] V.V. Meretoja, T. Tirri, M. Malin, J.V. Seppala, T.O. Narhi, Ectopic bone formation in and soft-tissue response to P(CL/DLLA)/bioactive glass composite scaffolds, Clin. Oral Implants Res. 25 (2) (2014) 159–164.
[6] S.J. Shih, W.L. Tzeng, R. Jatnika, C.J. Shih, K.B. Borisenko, Control of Ag nano-particle distribution influencing bioactive and antibacterial properties of Ag-doped mesoporous bioactive glass particles prepared by spray pyrolysis, J. Biomed. Mater. Res. B Appl. Biomater. 103 (4) (2015) 899–907.
[7] D. Clupper, L. Hench, Bioactive response of Ag-doped tape cast Bioglass 45S5 following heat treatment, J. Mater. Sci. Mater. Med. 12 (12) (2001) 917–921.
[8] X. Chatzistavrou, S. Velamakanni, K. DiRenzo, A. Lefkelidou, J.C. Fenno, T. Kasuga, A.R. Boccaccini, P. Papagerakis, Designing dental composites with bioactive and bactericidal properties, Mater. Sci. Eng. C 52 (2015) 267–272.
[9] Y. Wang, X. Chatzistavrou, D. Faulk, S. Badylak, L. Zheng, S. Papagerakis, L. Ge, H. Liu, P. Papagerakis, Biological and bactericidal properties of Ag-doped bioactive glass in a natural extracellular matrix hydrogel with potential application in dentistry, Eur. Cell. Mater. 29 (2015) 342–355.
[10] J. Berger, M. Reist, J.M. Mayer, O. Felt, N.A. Peppas, R. Gurny, Structure and interactions in covalently and ionically crosslinked chitosan hydrogels for biomedical applications, Eur. J. Pharm. Biopharm. 57 (1) (2004) 19–34.
[11] S. Supper, N. Anton, N. Seidel, M. Riemenschnitter, C. Curdy, T. Vandamme, Thermosensitive chitosan/glycerophosphate-based hydrogel and its derivatives in pharmaceutical and biomedical applications, Expert Opin. Drug Deliv. 11 (2) (2014) 249–267.
[12] X. Chatzistavrou, O. Tsigkou, H.D. Amin, K.M. Paraskevopoulos, V. Salih, A.R. Boccaccini, Sol–gel based fabrication and characterization of new bioactive glass–ceramic composites for dental applications, J. Eur. Ceram. Soc. 32 (12) (2012) 3051–3061.
[13] A. Briso, V. Rahal, S. Mestrener, J. Dezan, Biological response of pulps submitted to different capping materials, Braz. Oral Res. 20 (3) (2006) 219–225.

[14] W. Qin, X. Gao, T. Ma, M.D. Weir, J. Zou, B. Song, Z. Lin, A. Schneider, H.H.K. Xu, Metformin enhances the differentiation of dental pulp cells into odontoblasts by activating AMPK signaling, J. Endod. (2018).

[15] L. Pavez, N. Tobar, C. Chacón, R. Arancibia, C. Martínez, et al., Chitosan-triclosan particles modulate inflammatory signaling in gingival fibroblasts, J. Periodont. Res. (2017).

[16] C.S. Karthik, H.M. Manukumar, A.P. Ananda, S. Nagashree, K.P. Rakesh, L. Mallesha, H.L. Qin, S. Umesha, P. Mallu, N.B. Krishnamurthy, Synthesis of novel benzodioxane midst piperazine moiety decorated chitosan silver nanoparticle against biohazard pathogens and as potential anti-inflammatory candidate: a molecular docking studies, Int. J. Biol. Macromol. 108 (2018) 489–502.

[17] R. Arancibia, C. Maturana, D. Silva, N. Tobar, C. Tapia, Effects of chitosan particles in periodontal pathogens and gingival fibroblasts, J. Dent. Res. 92 (8) (2013) 740–745.

[18] L. Pavez, N. Tobar, C. Chacon, R. Arancibia, C. Martinez, C. Tapia, A. Pastor, M. Gonzalez, J. Martinez, P.C. Smith, Chitosan-triclosan particles modulate inflammatory signaling in gingival fibroblasts, J. Periodontal Res. Suppl. (2017).

[19] J. IN.Rôças Jr, J. Provenzano, F. Daibert, M. Bbs, Relationship between Fcγ receptor and interleukin-1 gene polymorphisms and post-treatment apical periodontitis, J. Endodontics 35 (9) (2009) 1186.

[20] X. Cheng, Y. Shen, R. Li, Targeting TNF: a therapeutic strategy for Alzheimer's disease, Drug Discov. Today 19 (11) (2014) 1822–1827.

[21] J. Kim, L. Gu, L. Breschi, L. Tjäderhane, K. Choi, Implication of ethanol wet-bonding in hybrid layer remineralization, J. Dent. Res. 89 (6) (2010) 575.

[22] X. Chatzistavrou, J.C. Fenno, D. Faulk, S. Badylak, T. Kasuga, A.R. Boccaccini, P. Papagerakis, Fabrication and characterization of bioactive and antibacterial composites for dental applications, Acta Biomater. 10 (8) (2014) 3723–3732.

[23] G. Jung, Y. Park, J. Han, Effects of HA released calcium ion on osteoblast differentiation, J. Mater. Sci. Mater. Med. 21 (5) (2010) 1649–1654.

[24] L. Hench, The story of Bioglass, J. Mater. Sci. Mater. Med. 17 (11) (2006) 967–978.

[25] X. Zhou, F. Moussa, S. Mankoci, P. Ustriyana, N. Zhang, Orthosilicic acid, Si(OH) 4, stimulates osteoblast differentiation in vitro by upregulating miR-146a to antagonize NF-κB activation, Acta Biomater. 39 (2016) 192–202.

[26] A.W. Wren, P. Hassanzadeh, L.M. Placek, T.J. Keenan, A. Coughlan, L.R. Boutelle, M.R. Towler, Silver nanoparticle coated bioactive glasses—composites with Dex/CMC hydrogels: characterization, solubility, and in vitro biological studies, Macromol. Biosci. 15 (8) (2015) 1146–1158.

[27] F. Pishbin, V. Mourino, J.B. Gilchrist, D.W. McComb, S. Kreppel, V. Salih, M.P. Ryan, A.R. Boccaccini, Single-step electrochemical deposition of antimicrobial orthopaedic coatings based on a bioactive glass/chitosan/nano-silver composite system, Acta Biomater. 9 (7) (2013) 7469–7479.

[28] C. Ma, Q. Wei, B. Cao, X. Cheng, J. Tian, H. Pu, A. Yusufu, L. Cao, A multifunctional bioactive material that stimulates osteogenesis and promotes the vascularization bone marrow stem cells and their resistance to bacterial infection, PLoS One 12 (3) (2017) e0172499.